Impact of hybrid nanoparticle reinforcements on mechanical properties of Epoxy-Polylactic Acid (PLA) Composites

K. Dileep, A. Srinath
Department of Mechanical Engineering, Koneru Lakshmaiah Education Foundation, KL Deemed to be University, Green Fields, Vaddeswaram, Guntur-522 502, India.
dileep.kotte@gmail.com, https://orcid.org/0000-0002-9279-2548
srinath@kluniversity.in, https://orcid.org/0000-0001-6284-256X

N.R. Banapurmath, M. A. Umarfarooq*, Ashok M. Sajjan
Centre of Excellence in Material Science, School of Mechanical Engineering, K.L.E. Technological University, BVB campus, Hubballi-580031, India
nr_banapurmath@kletech.ac.in, https://orcid.org/0000-0002-1280-6234
umarfarooq.ma@gmail.com, https://orcid.org/0000-0002-9369-7913
am_sajjan@kletech.ac.in, https://orcid.org/0000-0003-1251-8803

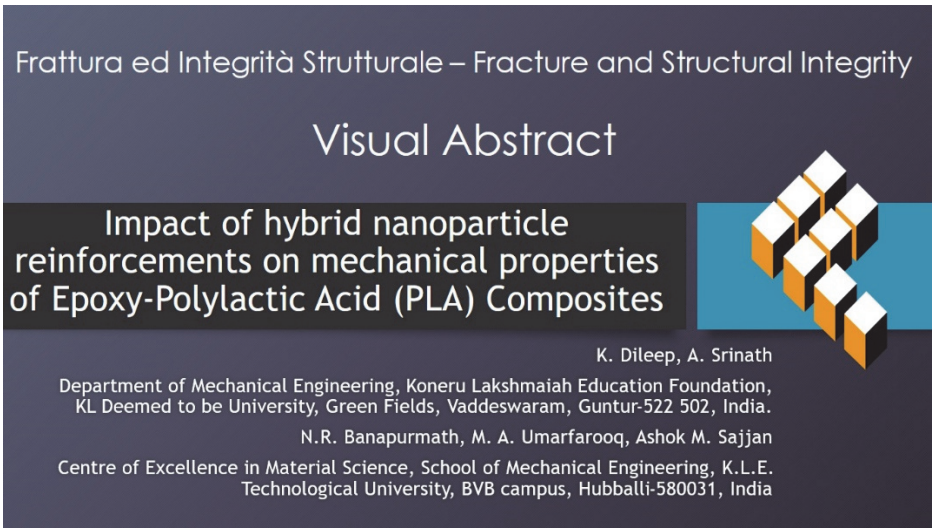

Citation: Dileep, K., Srinath, A., Banapurmath, N. R., Umarfarooq, M. A., Sajjan, A. M., Impact of hybrid nanoparticle reinforcements on Mechanical properties of Epoxy-Polylactic Acid (PLA) Composites, Frattura ed Integrità Strutturale, 70 (2024) 91-104.

Received: 29.05.2024
Accepted: 08.08.2024
Published: 12.08.2024
Issue: 10.2024

KEYWORDS. Hybrid nanocomposites, Mechanical testing, SEM.

INTRODUCTION

Synthetic and biopolymer-based materials play a role because of their many valuable properties. These polymers, such as epoxy resins polyimides and polyethylene, are known for their excellent strength-to-weight ratio, especially when compared to conventional materials like metals and ceramics [1-2]. The shift towards eco materials is necessary as petroleum resources become scarce and environmental pollution concerns grow. Nanocomposites have been widely

considered and studied by the researchers. Scientists are exploring different techniques to ensure that nanofillers are evenly distributed within the holding matrix for practical applications. With their extraordinary reliability and remarkable structural, electrical, and mechanical properties, polymer-based composites are demonstrated to be promising materials for a wide range of technical applications [3-6]. In materials science, it's fascinating to see how more significant quantities of GNP and amine-functionalized graphene nanocomposites can significantly improve mechanical properties compared to non-functionalized graphene material. Compared to raw epoxy, the amine-functionalized nanocomposites exhibited enhanced tensile strength but were relatively more delicate. There is a consequence of GNPs aggregation [7]. Graphene, a crystalline carbon allotrope, has a two-dimensional (2D) honeycomb structure of sp2 hybridized carbon atoms in a single monolayer sheet. According to all measurements, it is the universe's thinnest yet most potent material. Graphene has shown significant characteristics in terms of mechanical strength, ultra-large surface area, heat conductivity, fast electron mobility, and high current density, being the lightest and thinnest sp2 carbon nanomaterial. Because of their properties, perfect graphene applications are nanodevices and nanocomposites [8]. A study by Chang [9] examined the effect of carbon and glass fiber-reinforced composites and the addition of MWCNTs. Adding MWCNTs resulted in a substantial enhancement in both tensile strength (34.7%) and flexural strength (22.16%). In a research study, Ayatollahi et al. [10] examined the impact of the aspect ratio of MWCNT on the electrical and mechanical properties of epoxy/MWCNT composite plates. The aspect ratio has been found to affect the electrical and mechanical properties of nanocomposite materials greatly. Smaller MWCNTs have shown to possess significantly better qualities in this regard.

Nevertheless, according to a study by Wong et al. [11], the higher concentration of MWCNTs in polystyrene resin negatively impacts the tensile strength, tensile modulus, and failure strain. Therefore, it is crucial to determine the ideal weight percentage of nanoparticles to be incorporated into the resin system. This will significantly improve the mechanical properties of the composite materials. GNPs are a great option because they are cost-effective and can be produced in large quantities [12].

Our research focuses on studying the impact of hybrid nanofillers on the mechanical and fracture properties of Epoxy-PLA composite. The nanocomposites are studied by preparing epoxy-PLA composites with varying concentrations of hybrid fillers. Experimental results were compared with the findings from numerical analysis to investigate the impact of filler addition on tensile and bending strength.

EXPERIMENTAL DETAILS

Materials

A blend of an epoxy resin (Lapox-L12 and K6 hardener) and PLA added in the ratio of 80:20 is used as a matrix in this study. The epoxy and hardener were procured from Atul India Ltd, Gujarat, India. Additionally, the PLA granules are obtained from Nature Tech India Pvt. Ltd. The filler materials employed in this study are provided in Tab. 1, comprising SiO_2, GNPs, and MWCNTs.

Characteristic Property	SiO_2	GNPs	MWCNTs
Diameter (nm)	10-20	-	25
Thickness (nm)	-	3-6	-
Length/width (μm)	-	5-10	10
Density (g/cm^3)	2.4	0.24	0.24
Tensile Strength (MPa)	100	5000	5000
Tensile Modulus (GPa)	70	1000	1000
Poisson coefficient	0.15 [13]	0.19 [14]	0.3125 [15]
Purity (%)	99.5	> 99	> 99

Table 1: Properties of nanofillers.

Preparation of nanocomposites

For this study, a total of nine distinct nanocomposite samples were created. Fig. 1 depicts the procedure for fabricating nanocomposites. The PLA solution was prepared by dispersing PLA granules in a Tetrahydrofuran (THF) solution [16-17] and stirring it for 24 hours. The PLA solution was then combined with preheated epoxy and continuously stirred for 24 hours. The fillers were subsequently incorporated into the PLA-epoxy solution, which had undergone manual mixing for approximately 5 minutes before undergoing cold bath sonication at 40 kHz for approximately 50 minutes. After sonication, the K-6 hardener was added to the filler-loaded solution and gently swirled for five minutes. Finally, the resulting solution is cast into a mold and left to cure for 24 hours at room temperature. The composition of the nanocomposites prepared is provided in Tab. 2.

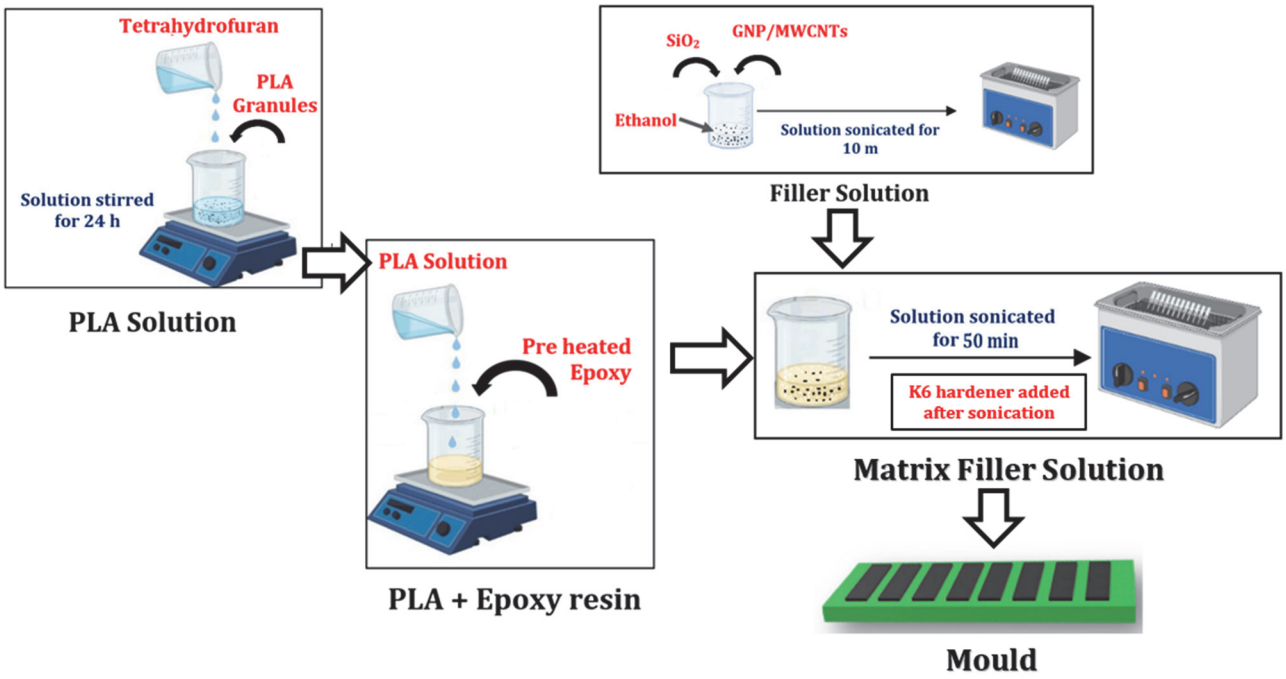

Figure 1: Nanocomposites preparation steps.

Serial No.	Specimen Code	Epoxy, wt.%	PLA, wt.%	SiO_2 wt.%	GNPs wt.%	MWCNTs wt.%
1	PE	80	20	-	-	-
2	ESG1	79.9	20	0.05	0.05	-
3	ESG2	79.8	20	0.10	0.10	-
4	ESG3	79.7	20	0.15	0.15	-
5	ESG4	79.6	20	0.20	0.20	-
6	ESM1	79.9	20	0.05	-	0.05
7	ESM2	79.8	20	0.10	-	0.10
8	ESM3	79.7	20	0.15	-	0.15
9	ESM4	79.6	20	0.20	-	0.20

Table 2: Composition of Epoxy-PLA blends and their nanocomposite.

COMPOSITE CHARACTERIZATION TESTS

Fourier transform infrared (FTIR) spectroscopy

The FTIR was conducted with a Perkin Elmer System series 2000 spectrophotometer, covering a wavenumber range from 3900 to 500 cm^{-1}. This was done to characterize the functional groups in SiO_2, MWCNTs/GNP loaded nanocomposites.

X-ray diffraction (XRD) spectroscopy

The XRD analysis of the epoxy composites (PE, ESG1, and ESM1) was conducted using a Rigaku SmartLab diffractometer, scanning from 5^0 to 90^0 at 2^0 per minute.

Tensile test

The tensile strength of the different specimens was evaluated using a Tinius Olsen UTM with a load cell capacity of 10 kN, following the guidelines of ASTM D 638 [18]. The experiments were conducted with a crosshead speed of 3 mm/min. Fig. 2 provides the specifications of the tensile specimen. A total of 5 samples were tested in each category, and the tensile strength was determined by calculating the average result.

Flexural test

The flexural strength was evaluated using a 3-point bending test according to the ASTM D 790 [19] using Tinius Olsen UTM (10kN capacity) with a 3 mm/min crosshead speed. The dimensions of the flexural specimen are shown in Fig. 2, with a span length of 80 mm. Five samples were tested within every category, and the average value was used to determine the flexural strength of the composite samples.

Impact test

The Izod impact test was conducted on an unnotched specimen using a pendulum impact tester (Zwick/Roell Hit 50p model) according to ASTM D4812 [20]. The test was performed with a calculated theoretical impact velocity of 3.458 $m.s^{-1}$. Fig. 2 illustrates the dimensions of the specimen employed in this test.

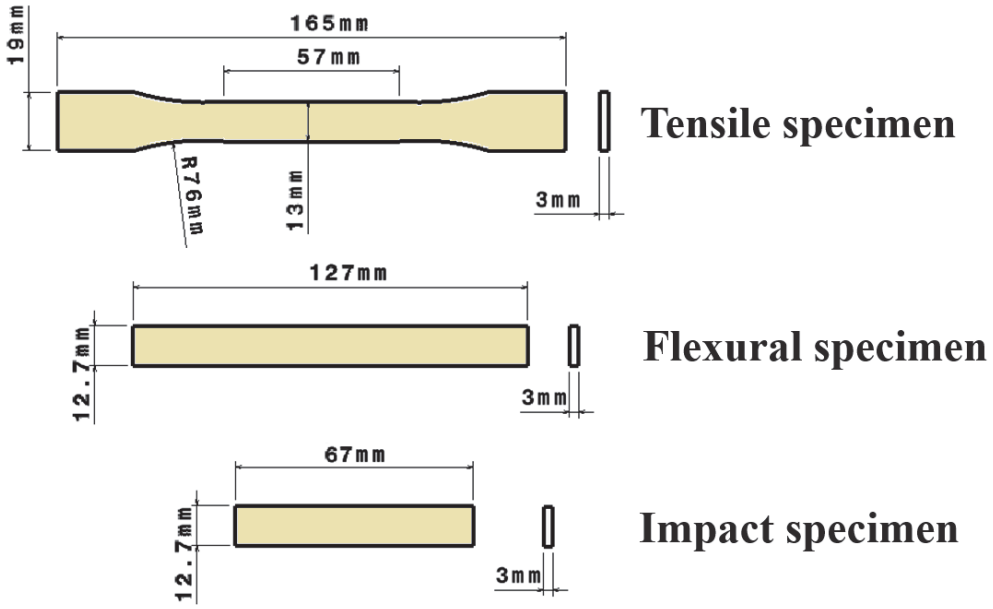

Figure 2: Dimensions of specimens for mechanical testing.

RESULTS AND DISCUSSIONS

FTIR findings

Fig. 3 depicts the FTIR spectra of three different materials: PE, ESG1, and ESM1. In the PE sample, peaks at 2931 cm^{-1}, signifying C-H stretching, and at 2964 cm^{-1}, indicating -CH2 stretching vibration can be observed. Furthermore, the strength of specific peaks in PE decreases due to the interaction between the epoxy groups and the PLA COOH groups [21].

Aside from the spectra in the PE composite, two additional characteristics are seen in ESG1 and ESM1 composites. First, a stretching signal at around 1050 cm^{-1} develops, which matches Si-O-Si stretching. Second, a prominent peak at 2900 cm^{-1} shows C-H stretching. A C=C stretching peak is also found at roughly 1600 cm^{-1}, confirming the presence of carbon-based nanofillers, notably GNP and MWCNT [22-23]. This shows that the fillers and matrix material interact more effectively. These findings indicate the spectroscopic changes and interactions within the investigated materials.

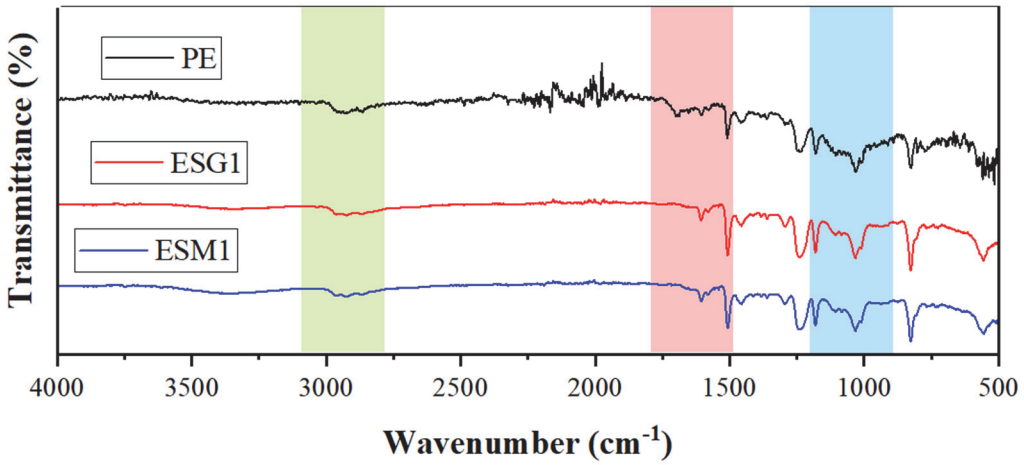

Figure 3: FTIR spectra of PE, ESM1 and ESG1.

XRD findings

The XRD patterns of the pure PE, ESG1, and ESM1 are presented in Fig. 4. The PE sample displayed broad peaks around $2\theta = 20^{0}$, indicating the amorphous nature, and a notable peak at $2\theta = 22.44^{0}$ [24], pointing to the epoxy's semi-crystalline regions. The ESM1 sample exhibited characteristic MWCNTs peaks at $2\theta = 26^{0}$ and 42^{0}, along with a SiO2 peak at $2\theta = 26.6^{0}$ [25], which confirms the effective incorporation of these nanofillers into the composite, contributing to its semi-crystalline structure. The ESG1 samples exhibited a prominent peak at $2\theta = 26^{0}$, suggestive of high-quality graphene sheets, and a similar peak at $2\theta = 26.6^{0}$ [26]. All samples showed a typical broad peak at $2\theta = 20^{0}$, representing the amorphous phase and semi-crystalline epoxy peak at $2\theta = 22.44^{0}$.

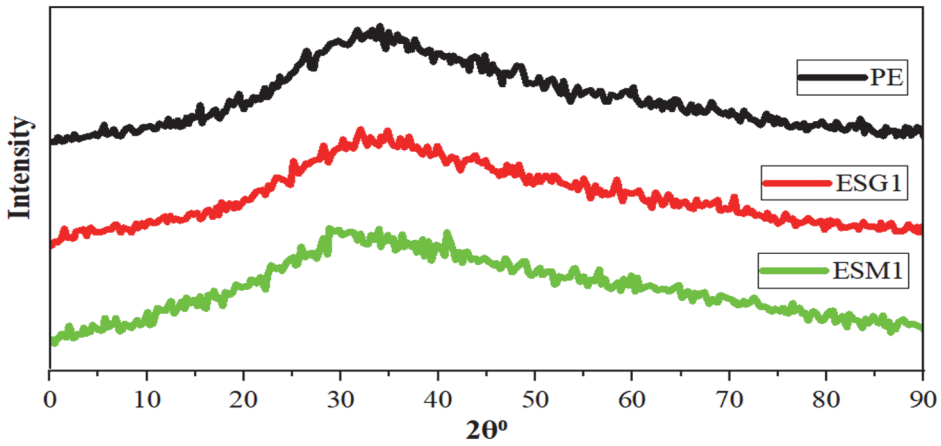

Figure 4: XRD spectra of PE, ESM1 and ESG1.

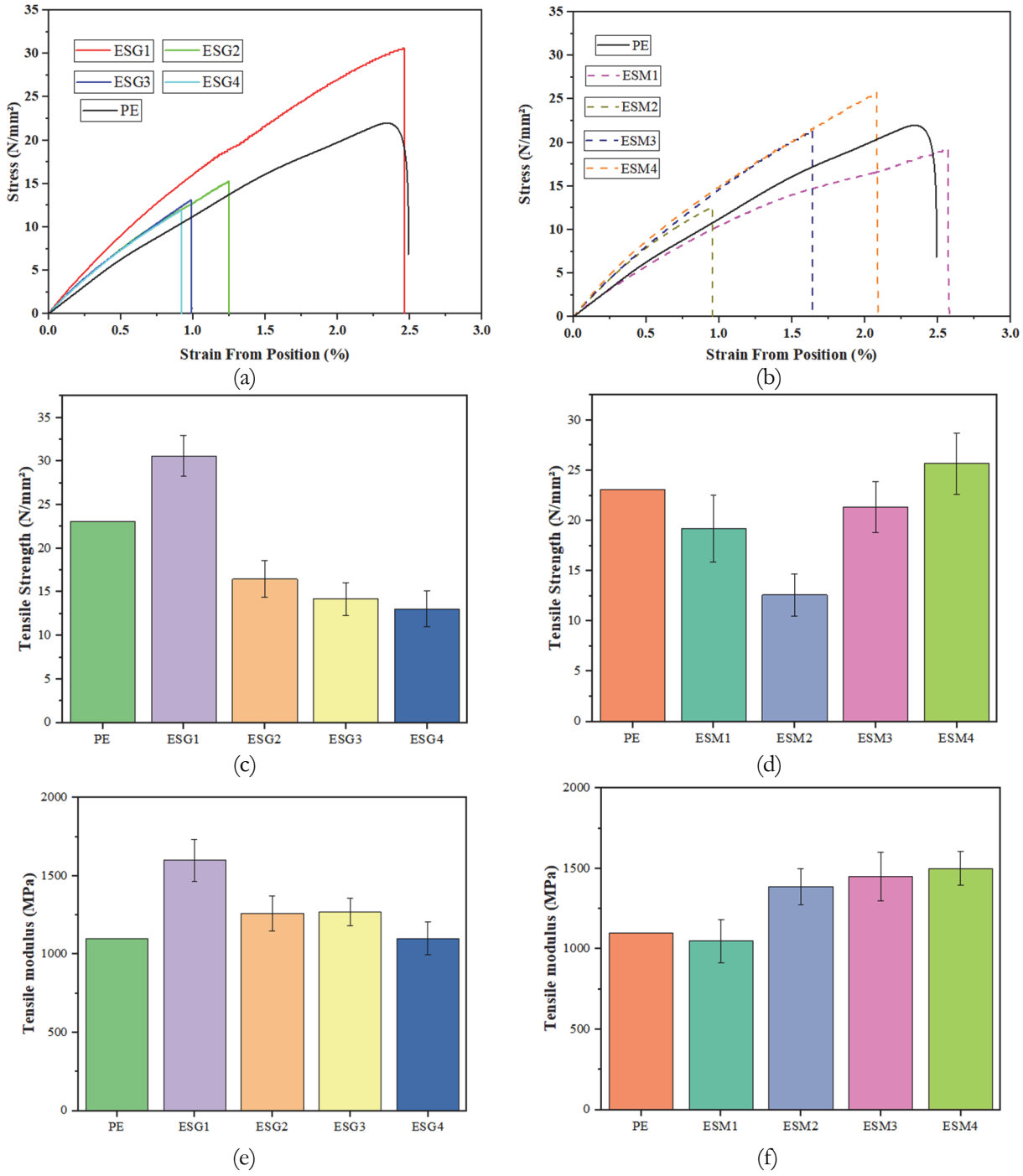

Figure 5: (a) Stress-strain curves of ESG1-4 compared with PE blend (b) Stress-strain curves of ESM1-4 compared with PE blend (c) Tensile strength of PE and ESG1-4 samples (d) Tensile strength of PE and ESM1-4 samples (e) Tensile modulus of PE and ESG1-4 samples (f) Tensile modulus of PE and ESM1-4 samples.

Tensile test results

The stress-strain curves of nanocomposites loaded with GNPs and MWCNTs are depicted in Figs. 5(a) and 4(b) correspondingly. Fig. 5(c)-5(f) presents the tensile strength and modulus of nanocomposites. The tensile strength of the PE sample was found to be 23.07 MPa, whereas the tensile strength of ESG1, ESG2, ESG3, and ESG4 was observed to be 30.61 MPa, 16.48 MPa, 14.18 MPa and 13.07 MPa respectively. An increase in strength was observed in ESG1, whereas nanocomposites loaded with higher concentrations exhibited a lower strength than PE composite. The PE composite had a tensile modulus of 1100 MPa. The tensile modulus of ESG1, ESG2, ESG3, and ESG4 was observed to be 1600 MPa, 1260 MPa, 1270 MPa, and 1100 MPa, respectively. ESG1 exhibited the highest tensile modulus at 1600 MPa, indicating that

the 0.1 wt% filler content results in the highest stiffness among the tested composites. The ESG1 material demonstrated a significant 33% enhancement in tensile strength and a 46% rise in tensile modulus.
ESM1, ESM2, ESM3, and ESM4 exhibited tensile strengths of 19.22 MPa, 12.61 MPa, 21.35 MPa, and 25.68 MPa, respectively. Notably, ESM4 demonstrated an 11.31% increase in tensile strength, while ESM1, ESM2, and ESM3 exhibited lower strengths than PE. The tensile moduli of the nanocomposites ESM1, ESM2, ESM3, and ESM4 were 1050 MPa, 1388 MPa, 1450 MPa, and 1500 MPa, respectively. Significantly, ESM4 exhibited a considerable 37% augmentation in modulus. The impact of the fillers on the tensile strength and tensile modulus of the composites was found to be minimal. Composites loaded with GNP and MWCNTs displayed distinct mechanical responses when subjected to tensile forces. Except for ESM4, which exhibited a marginal 11% increase in strength, the incorporation of MWCNTs and SiO_2 adversely impacted the tensile strength of the epoxy-PLA composite. Interestingly, there was a significant enhancement of up to 37% in the tensile modulus. Similarly, in composites loaded with GNP, only ESG1 demonstrated a higher strength (33%) than PE composite, while there was a notable increase of up to 46% in modulus. Once again, it should be noted that the correlation between filler content and tensile qualities, precisely strength and modulus, does not adhere strictly to a linear connection. The increase in strength and modulus of the nanocomposites can be attributed to the utilization of fillers with high strength and modulus.
Epoxy nanocomposites loaded with 0.1 wt% GNP outperform MWCNTs at the same weight. This is likely due to GNPs having higher specific surface area and increased nanofillers-matrix adhesion due to their rough surface. These factors lead to better stress transfer and higher tensile strength. In contrast, MWCNTs have a 1-dimensional tubular structure, which makes stress transfer more challenging compared to the planar structure of GNPs. The potential for aggregation and less effective interfacial adhesion in MWCNTs results in lower tensile strength and modulus improvements. [27-28].

SEM analysis

The purpose of the SEM analysis was to study the dispersion of fillers in the matrix and to observe the filler-matrix interaction [29-30]. The SEM analysis was carried out on the fractured samples from the tensile test. Fig. 6 shows SEM micrographs of the pure epoxy-PLA blend and their nanocomposites.
Fig. 6(b)-(e) shows SEM micrographs of GNPs nanocomposites. The fracture surface of the pure Epoxy-PLA (Plain) specimen depicted in Fig. 6(a) has a smooth texture, suggesting a typical brittle fracture pattern. Notably, no obvious cavities can be found on the surface of these produced materials. In contrast, the surfaces of the GNP-loaded samples (Fig. 6 (b)-(e)) seem rough, and cleavage planes are visible. Notably, the cleavage planes in the ESG1 samples are smaller than those in the ESG2, ESG3, and ESG4 samples. A higher number of cleavage planes equates to more sites capable of absorbing fracture energy, thus improving resistance to crack propagation.
As a result, the ESG1 had increased tensile strength and modulus comparable to SiO_2 and MWCNTs loaded nanocomposites (Fig. 6(f)-6(i)). The surface of ESM4 is rougher and has more cleavage planes than PE and other comparable nanocomposites. As a result, ESM4 has increased tensile strength and modulus.
The GNPs-loaded composites generally show finer and more numerous cleavage planes than MWCNTs composites, indicating better stress transfer and energy absorption. The planer structure of GNPs facilitates better interaction with the matrix, leading to higher tensile properties. On the other hand, MWCNTs, with their 1D tubular structure, show less defined features and potentially lower dispersion efficiency, resulting in varied mechanical enhancements [27-28].

Flexural test results

The flexural strength of nanocomposites loaded with GNPs and MWCNTs is depicted in Figs. 7(a) and 7(b) correspondingly. The results showed that adding fillers significantly influenced the flexural strength of the nanocomposites. The bending strength of the PE composite was found to be 51.7 MPa. The flexural strengths of ESG1, ESG2, ESG3, and ESG4 were 64.14 MPa, 49.16 MPa, 29.47 MPa, and 49.60 MPa, respectively. Adding a small amount (0.1 wt%) of SiO_2 and GNPs enhances flexural strength significantly compared to PE, suggesting effective reinforcement. However, an increase to 0.2 wt% results in a slight decrease, potentially indicating an optimal filler concentration. At 0.3 wt%, a significant drop in strength suggests an excess of fillers causing matrix disruption. Finally, at 0.4 wt%, the flexural strength remains similar to 0.2 wt%, implying that a saturation point may have been reached, highlighting the importance of precise filler content control for tailored material properties.
The flexural strengths of ESM1, ESM2, ESM3, and ESM4 were 37.66 MPa, 32.82 MPa, 39.27 MPa and 69.71 MPa respectively. ESM4 exhibited an increase in strength by 37 %, whereas ESM1-ESM3 composites exhibited lower strength than PE samples. Epoxy nanocomposites loaded with GNPs outperform MWCNTs due to their higher specific surface area and better matrix adhesion, leading to more efficient stress transfer. The 1D structure and potential accumulation of MWCNTs result in less effective interfacial adhesion and lower tensile strength improvements.

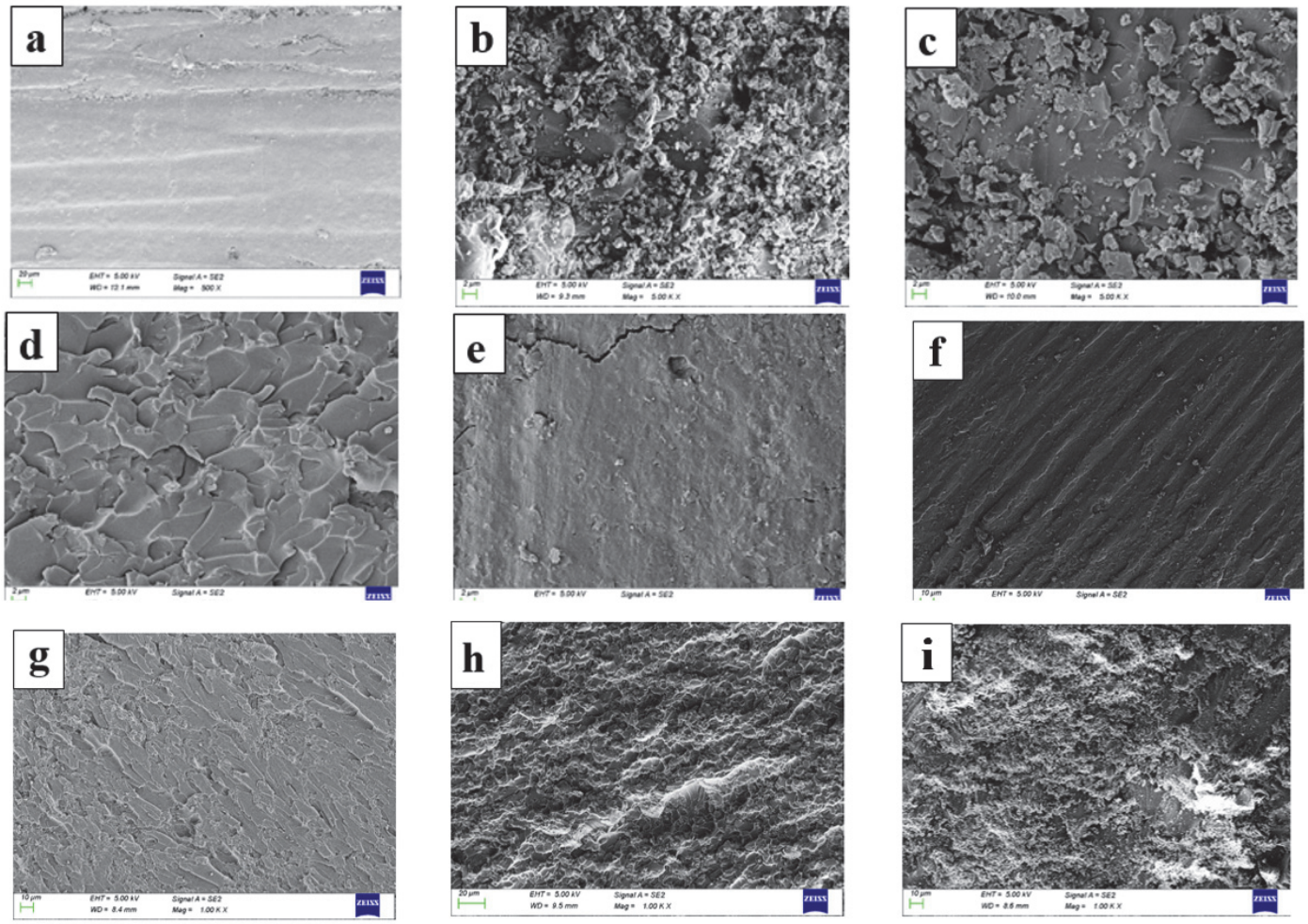

Figure 6: SEM images of fracture surfaces from tensile tests of (a) PE (b) ESG1 (c) ESG2 (d) ESG3 (e) ESG4 (f) ESM1 (g) ESM2 (h) ESM3 (i) ESM4.

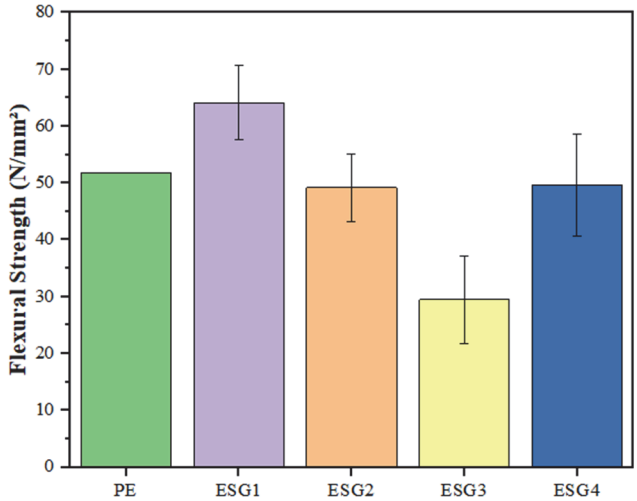

Figure 7(a): Flexural strength of PE and ESG1-4 samples.

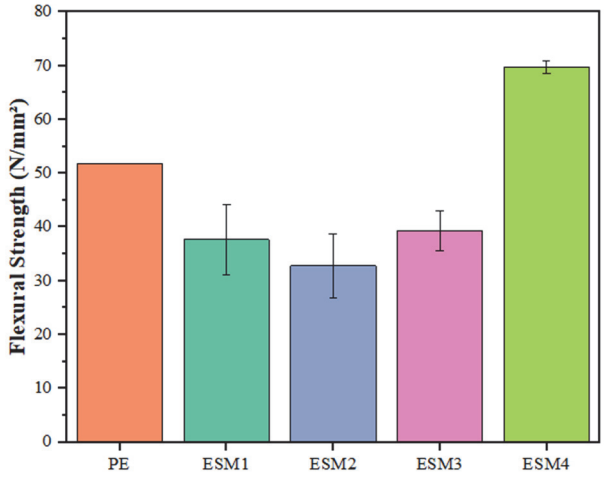

Figure 7(b): Flexural strength of PE and ESM1-4 samples.

Impact test analysis

Fig. 8 displays the impact strength results for the pristine Epoxy/PLA blend and their nanocomposites. The introduction of various fillers had a noteworthy influence on the impact resistance of these Epoxy/PLA nanocomposites. The initial impact strength of the PE blend was measured at 50.56 J/m.

Within the group of GNP composites, ESG1, ESG3, and ESG4 displayed impact strengths of 80.31 J/m, 69.41 J/m, and 64.98 J/m, respectively. All GNP-loaded composites, except for ESG2, exhibited higher impact strength than the PE composite, with ESG1 achieving the highest strength within this category.

On the other hand, the MWCNTs-loaded composites exhibited a distinct behavior when compared to the GNP-loaded composites. ESM1, ESM2, ESM3, and ESM4 composites showed impact strengths of 53.27 J/m, 29.05 J/m, 27.54 J/m, and 60.57 J/m, respectively. Similar to the tensile and flexural results of GNPs, loaded composites exhibited higher impact strength compared to MWCNTs added composites

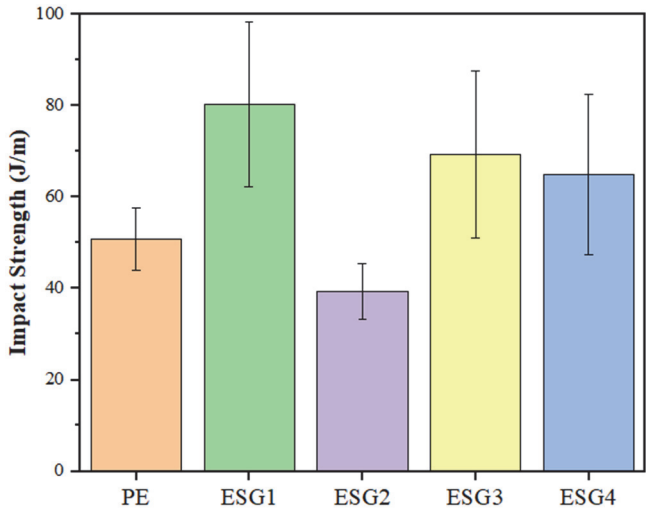

Figure 8(a): Impact strength of PE and ESG1-4 samples

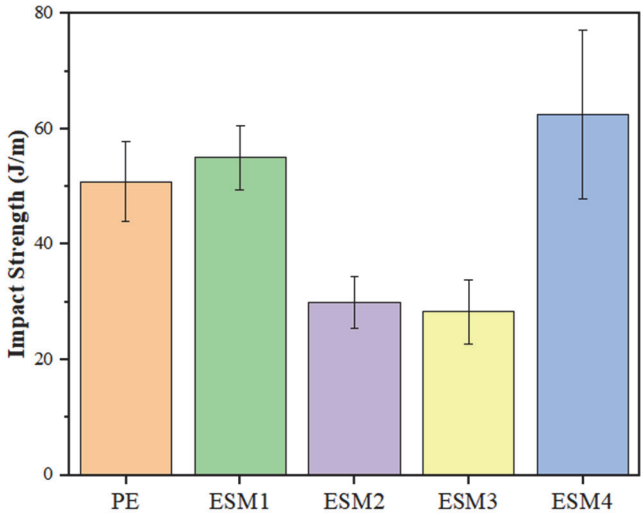

Figure 8(b): Impact strength of PE and ESM1-4 samples

SIMULATION STUDIES

Studies using simulation employ finite element (FE) analysis [31-32] to forecast mechanical properties, which are then confirmed through experimental findings.

Creating a material and three-dimensional model

A comprehensive two-step FE simulation methodology was adopted to thoroughly evaluate the influence of hybrid filler particles (SiO2/GNPs and SiO2/MWCNTs) on composite properties, employing an effective hybrid technique [17, 21, 33-34]. Fig. 9 illustrates the procedural framework of this simulation approach.

Step 1: In the first step, a representative volume element (RVE)of the nanocomposite is created in the Material designer module of ANSYS Workbench using the properties and weight fractions of the matrix and fillers (either GNPs or MWCNTs). The elastic constants of nanocomposite are obtained from this step.

Step 2: Again, using the RVE approach, the properties of the hybrid nanocomposites are determined by utilizing the established nanocomposite properties (From Step 1) as a revised matrix material, termed the effective matrix, and SiO_2 as filler material. The final properties of the hybrid nanocomposites are thus determined through this process of dual integration.

The three-dimensional model for the simulation of tensile and flexural tests was created using CATIA V5, following the dimensions provided in Fig. 2.

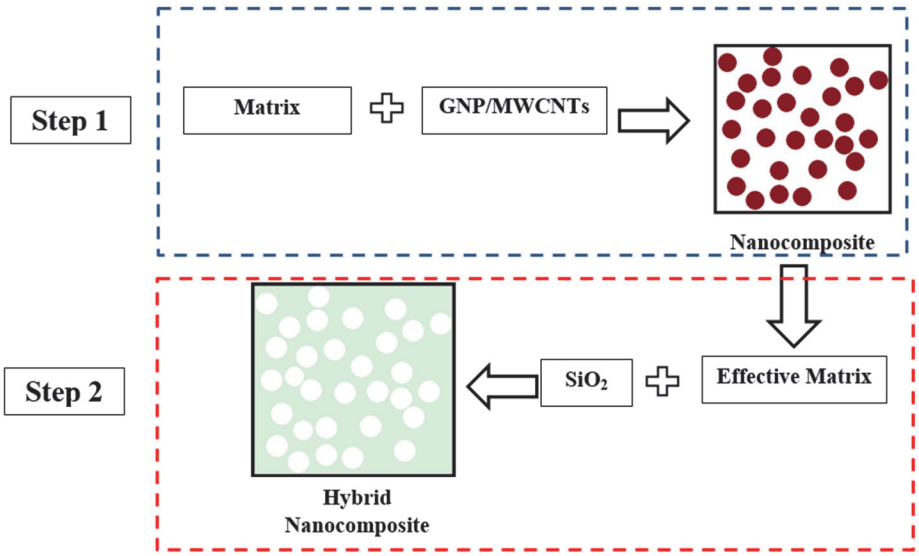

Figure 9: Procedure to determine properties of hybrid nanocomposite

Mesh generation and boundary conditions

Tensile and flexural models were meshed with Hex20 elements, as shown in Figs. 10(a) and 10(b). The boundary conditions applied to simulate the tensile and flexural test are shown in Figs. 11(a) and 11(b), respectively. One edge of the specimen is clamped securely when conducting tensile tests while axial force is applied to the other end. On the other hand, in flexural tests, the specimen is loaded at the center and supported at both ends.

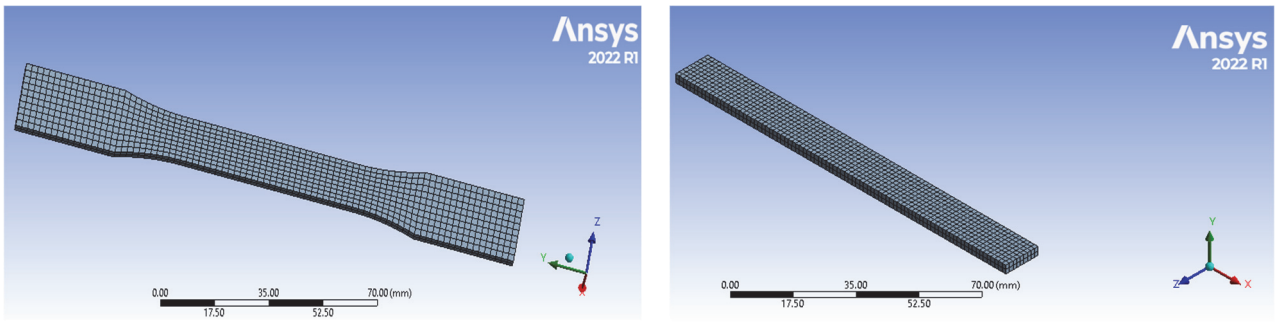

(a) (b)

Figure 10 (a) Tensile specimen after Meshing (b) Flexural specimen after Meshing

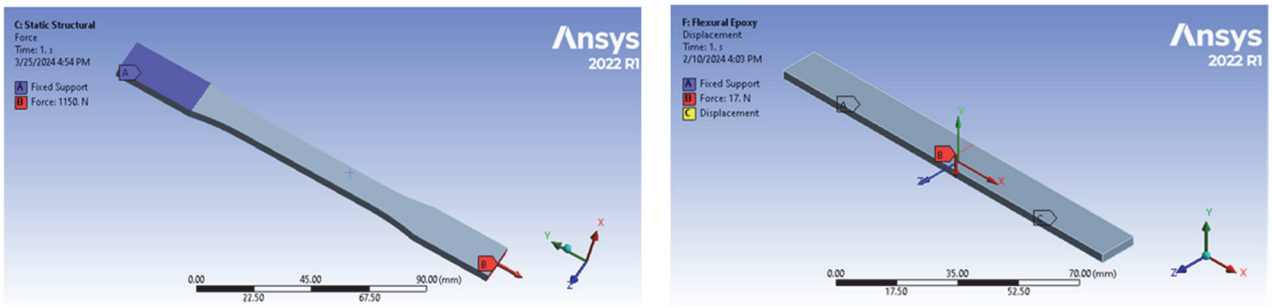

(c) (d)

Figure 11: Boundary conditions for simulation of (a) Tensile specimen (b) Flexural specimen.

SIMULATION RESULTS

The simulation was carried out under boundary conditions resembling those observed in the experimental outcomes. The maximum force values withstood by the specimen until failure were utilized as a reference for evaluating the simulation methods

When the S1 specimen was subjected to an axial force of around 1150 N in a tensile test, the equivalent von Mises stress closely matched the experimental data, as illustrated in Fig. 12(a), consistent with the physical test plots (Fig. 5(a)). Similarly, in simulating a 3-point flexural test for the S1 specimen, a vertical load of 17 N was applied at the center, with the corresponding variation of equivalent stress depicted in Fig. 12(b). Tab. 3 compares the tensile and flexural strengths for all specimens derived from experimentation and FE simulation. The disparities between the experimental and simulated tensile and flexural strengths were within 11%.

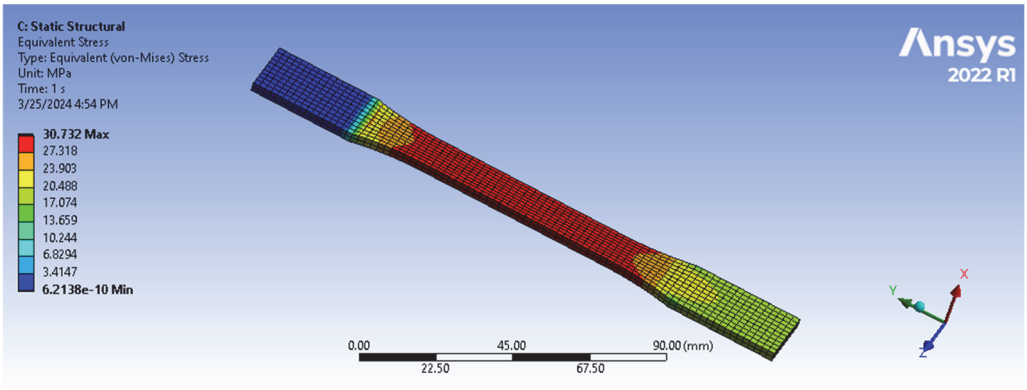

(a)

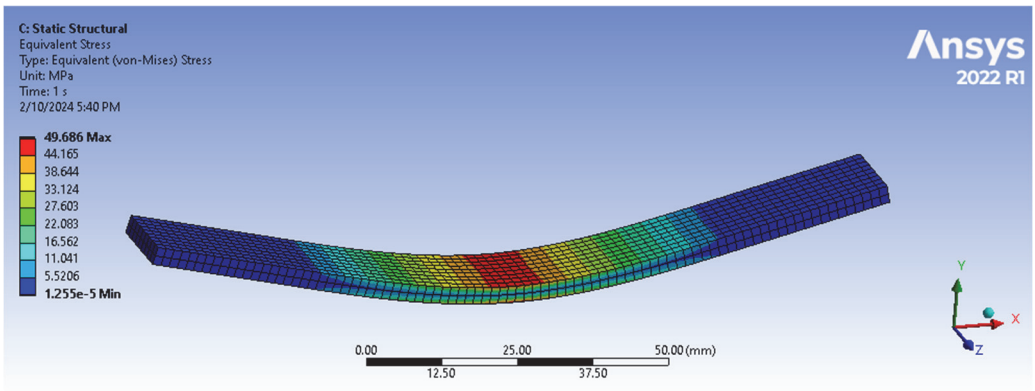

(b)

Figure 12: Max. equivalent stress in the S1 specimen under (a) Tensile load (b) Bending load.

CONCLUSIONS

This study investigated the influence of incorporating SiO_2/GNPs and SiO_2/MWCNTs on the mechanical properties of epoxy-PLA composites. The composites were prepared with varying concentrations of hybrid fillers (0.1 to 0.4 wt. % for each filler) using a combination of bath sonication and hand-casting techniques. The results demonstrated that ESG1, with a composition of 0.05 wt% SiO_2 and 0.05 wt% GNPs, exhibited significant enhancements in tensile, flexural, and impact strength with increases of 33%, 24%, and 59%, respectively, compared to the epoxy-PLA blend. However, higher filler concentrations did not consistently perform satisfactorily in all tests. However, ESM4 (0.5 wt% SiO_2 + 0.2 wt% MWCNTs) showed a noticeable improvement in tensile, flexural, and impact strength, increasing 11%, 34%, and 20%. Epoxy nanocomposites with GNPs exhibit higher tensile strength than those with MWCNTs due to better stress transfer from higher specific surface area and improved matrix adhesion. At the same time, MWCNTs face challenges like potential agglomeration and less effective interfacial adhesion. The experimental results were corroborated by

numerical analysis, showing a close agreement in the tensile and bending strength of the nanocomposites. Overall, the study highlights the potential of hybrid fillers to enhance the mechanical properties of epoxy-PLA composites, with optimal filler content vital for maximizing these improvements.

Serial No.	Specimen Code	Tensile strength (MPa)			Flexural strength (MPa)		
		From simulation	From experimental results	Variation in results (%)	From simulation	From experimental results	Variation in results (in %)
1	PE	23.87	23.07	3.47	52.87	51.7	2.26
2	ESG1	30.73	30.61	0.39	49.69	49.17	1.06
3	ESG2	17.97	16.48	9.04	63.10	64.15	1.64
4	ESG3	15.28	14.18	7.76	30.00	29.47	1.80
5	ESG4	15.78	13.07	10.79	49.66	49.62	0.08
6	ESM1	21.33	19.22	10.98	18.62	18.83	1.12
7	ESM2	14.67	12.61	8.41	17.59	16.41	7.19
8	ESM3	23.15	21.35	8.43	19.35	19.63	-1.43
9	ESM4	27.88	25.68	8.57	36.08	34.86	3.50

Table 3: Comparison of Tensile and Flexural strengths of all specimens obtained from experimentation and FE Simulation.

REFERENCES

[1] Gouda, P.S., Sridhar, I. and Umarfarooq, M.A. (2022). Crack suppression in glass epoxy hybrid L-bend composites through drawdown coating technique using nano and micro fillers. Materials Today: Proceedings, 62, pp. 7292-7296. DOI: 10.1016/j.matpr.2022.04.465.

[2] Parveez, B., Kittur, M.I., Badruddin, I.A., Kamangar, S., Hussien, M. and Umarfarooq, M.A. (2022). Scientific Advancements in Composite Materials for Aircraft Applications: A Review. Polymers, 14(22), p. 5007. DOI: 10.3390/polym14225007.

[3] Xiong, R., Grant, A.M., Ma, R., Zhang, S. and Tsukruk, V.V. (2018). Naturally-derived biopolymer nanocomposites: Interfacial design, properties, and emerging applications. Materials Science and Engineering: R: Reports, 125, pp.1-41. DOI: 10.1016/j.mser.2018.01.002.

[4] Feng, P., Kong, Y., Yu, L., Li, Y., Gao, C., Peng, S., Pan, H., Zhao, Z. and Shuai, C. (2019). Molybdenum disulfide nanosheets embedded with nanodiamond particles: co-dispersion nanostructures as reinforcements for polymer scaffolds. Applied Materials Today, 17, pp. 216-226. DOI: 10.1016/j.apmt.2019.08.005.

[5] Taibi, N., Belabed, Z., Boucham, B., Benguediab, M., Tounsi, A., Khedher, K.M. and Salem, M.A. (2024). On the Thermomechanical Behavior of Laminated Composite Plates using different Micromechanical-based Models for Coefficients of Thermal Expansion (CTE). Journal of Applied and Computational Mechanics, 10(2), pp. 224-244. DOI: 10.22055/jacm.2023.44257.4191.

[6] Slimani, O., Belabed, Z., Hammadi, F., Taibi, N. and Tounsi, A. (2021). A new shear deformation shell theory for free vibration analysis of FG sandwich shells. Structural Engineering and Mechanics, An Int'l Journal, 78(6), pp. 739-753. DOI: 10.12989/sem.2021.78.6.739.

[7] Salom, C., Prolongo, M.G., Toribio, A., Martínez-Martínez, A.J., de Cárcer, I.A. and Prolongo, S.G. (2018). Mechanical properties and adhesive behaviour of epoxy-graphene nanocomposites. International Journal of Adhesion and Adhesives, 84, pp. 119-125. DOI: 10.1016/j.ijadhadh.2017.12.004.

[8] Bahadır, E.B. and Sezgintürk, M.K. (2016). Applications of graphene in electrochemical sensing and biosensing. TrAC Trends in Analytical Chemistry, 76, pp. 1-14. DOI: 10.1016/j.trac.2015.07.008.

[9] Chang, M.S. (2010). An investigation on the dynamic behaviour and thermal properties of MWCNTs/FRP laminate composites. Journal of Reinforced Plastics and Composites, 29(24), pp. 3593-3599. DOI: 10.1177/0731684410379510.
[10] Ayatollahi, M.R., Shadlou, S., Shokrieh, M.M. and Chitsazzadeh, M. (2011). Effect of multi-walled carbon nanotube aspect ratio on mechanical and electrical properties of epoxy-based nanocomposites. Polymer Testing, 30(5), pp. 548-556. DOI: 10.1016/j.polymertesting.2011.04.008.
[11] Wong, M., Paramsothy, M., Xu, X.J., Ren, Y., Li, S. and Liao, K. (2003). Physical interactions at carbon nanotube-polymer interface. Polymer, 44(25), pp. 7757-7764. DOI: 10.1016/j.polymer.2003.10.011.
[12] Cataldi, P., Athanassiou, A. and Bayer, I.S. (2018). Graphene nanoplatelets-based advanced materials and recent progress in sustainable applications. Applied Sciences, 8(9), p.1438. DOI: /10.3390/app8091438.
[13] Greaves, G.N., Greer, A.L., Lakes, R.S. and Rouxel, T. (2011). Poisson's ratio and modern materials. Nature materials, 10(11), pp. 823-837. DOI: 10.1038/nmat3134.
[14] Rouway, M., Nachtane, M., Tarfaoui, M., Chakhchaoui, N., Omari, L.E.H., Fraija, F. and Cherkaoui, O. (2021). Mechanical properties of a biocomposite based on carbon nanotube and graphene nanoplatelet reinforced polymers: Analytical and numerical study. Journal of Composites Science, 5(9), p.234. DOI: 10.3390/jcs5090234.
[15] Li, C. and Chou, T.W. (2003). Elastic moduli of multi-walled carbon nanotubes and the effect of van der Waals forces. Composites Science and Technology, 63(11), pp. 1517-1524. DOI: 10.1016/S0266-3538(03)00072-1.
[16] Dileep, K., Srinath, A., Banapurmath, N.R., Umarfarooq, M.A. and Sajjan, A.M. (2023). Mechanical and Fracture Characterization of Epoxy/PLA/Graphene/SiO_2 Composites. Frattura ed Integrità Strutturale, 17(64), pp. 229-239. DOI: 10.3221/IGF-ESIS.64.15.
[17] Nimbagal, V., Banapurmath, N.R., Umarfarooq, M.A., Revankar, S., Sajjan, A.M., Soudagar, M.E.M., Shahapurkar, K., Alamir, M.A., Alarifi, I.M. and Elfasakhany, A. (2023). Mechanical and fracture properties of carbon nano fibers/short carbon fiber epoxy composites. Polymer Composites. DOI: 10.1002/pc.27371.
[18] ASTM D638-14:2014. Standard Test Method for Tensile Properties of Plastics; ASTM International: West Conshohocken, PA, USA, (2014).
[19] ASTM D790. Standard test methods for flexural properties of unreinforced and reinforced plastics and electrical insulating materials. West Conshohocken, PA: ASTM International, (2010).
[20] ASTM D4812-11, Standard Test Method for Unnotched Cantilever Beam Impact Resistance of Plastics.
[21] Revankar, S., Banapurmath, N.R., Sajjan, A.M., Nimbagal, V., Patil, A.Y., Venkatesh, R., Umarfarooq, M.A., Vadlamudi, C. and Krishnappa, S. (2022). Epoxy-poly lactic acid blended composites reinforced with carbon fibres for engineering applications. Materials Express, 12(12), pp. 1502-1511. DOI: 10.1166/mex.2022.2303.
[22] Chieng, B.W., Ibrahim, N.A., Wan Yunus, W.M.Z. and Hussein, M.Z. (2013). Poly(lactic acid)/poly(ethylene glycol) polymer nanocomposites: Effects of graphene nanoplatelets. Polymers, 6(1), pp. 93–104. DOI: 10.3390/polym6010093.
[23] Ibrahim Lakin, I., Abbas, Z., Azis, R.S., Ibrahim, N.A. and Abd Rahman, M.A. (2020). The Effect of MWCNTs Filler on the Absorbing Properties of OPEFB/PLA Composites Using Microstrip Line at Microwave Frequency. Materials, 13(20), p.4581. DOI: 10.3390/ma13204581
[24] Ho, M.W., Lam, C.K., Lau, K.T., Ng, D.H. and Hui, D. (2006). Mechanical properties of epoxy-based composites using nanoclays. Composite structures, 75(1-4), pp. 415-421. DOI: 10.1016/j.compstruct.2006.04.051.
[25] Imani, A., Arabi, M. and Farzi, G. (2016). Effect of in-situ oxidative preparation on electrical properties of Epoxy/PANi/MWCNTs nanocomposites. Journal of Materials Science: Materials in Electronics, 27, pp. 10364-10370. DOI: 10.1007/s10854-016-5122-0.
[26] Pang, J. and Yeming, W. (2018). Graphene oxide on the microstructure and mechanical properties of cement based composite material. Frattura ed Integrità Strutturale, 12(45), pp. 156-163. DOI: 10.3221/IGF-ESIS.45.13.
[27] Rafiee, M.A., Rafiee, J., Wang, Z., Song, H., Yu, Z.Z. and Koratkar, N. (2009). Enhanced mechanical properties of nanocomposites at low graphene content. ACS nano, 3(12), pp. 3884-3890. DOI: 10.1021/nn9010472.
[28] Mittal, G., Dhand, V., Rhee, K.Y., Park, S.J. and Lee, W.R. (2015). A review on carbon nanotubes and graphene as fillers in reinforced polymer nanocomposites. Journal of industrial and engineering chemistry, 21, pp. 11-25. DOI: https:10.1016/j.jiec.2014.03.022.
[29] Zakaria, M.R., Kudus, M.H.A., Akil, H.M. and Thirmizir, M.Z.M. (2017). Comparative study of graphene nanoparticle and multiwall carbon nanotube-filled epoxy nanocomposites based on mechanical, thermal and dielectric properties. Composites Part B: Engineering, 119, pp. 57-66. DOI:10.1016/j.compositesb.2017.03.023.
[30] Singh, S., Srivastava, V.K. and Prakash, R. (2015). Influences of carbon nanofillers on the mechanical performance of epoxy resin polymer. Applied Nanoscience, 5, pp. 305-313. DOI: 10.1007/s13204-014-0319-0.

[31] Mesbah, A., Belabed, Z., Tounsi, A., Ghazwani, M.H., Alnujaie, A. and Aldosari, S.M. (2024). Assessment of New Quasi-3D Finite Element Model for Free Vibration and Stability Behaviors of Thick Functionally Graded Beams. Journal of Vibration Engineering & Technologies, 12(2), pp. 2231-2247. DOI: 10.1007/s42417-023-00976-8.

[32] Belabed, Z., Tounsi, A., Bousahla, A.A., Tounsi, A. and Yaylacı, M. (2024). Accurate free and forced vibration behavior prediction of functionally graded sandwich beams with variable cross-section: A finite element assessment. Mechanics Based Design of Structures and Machines, pp. 1-34. DOI:10.1080/15397734.2024.2337914.

[33] Ervina, J., Mariatti, M. and Hamdan, S. (2016). Effect of filler loading on the tensile properties of multi-walled carbon nanotube and graphene nanopowder filled epoxy composites. Procedia Chemistry, 19, pp. 897-905. DOI: 10.1016/j.proche.2016.03.132.

[34] Shokrian, M.D., Shelesh-Nezhad, K. and H Soudmand, B. (2017). Numerical simulation of a hybrid nanocomposite containing Ca-CO3 and short glass fibers subjected to tensile loading. Mechanics of Advanced Composite Structures, 4(2), pp. 117-125. DOI:10.22075/macs.2017.1772.1092.